ASSESSMENT OF LAND DEFORMATION AND LAND USE RELATIONSHIP IN GARMSAR ALLUVIAL FAN USING SENTINEL-1 DATA

F. Rafiei [1], S. Gharechelou [2]*, M. Hosseinpoor [1]

[1] Dept. of Water and Environment, Faculty of Civil Engineering, Shahrood University of Technology, Iran – Fateme_rafiei@outlook.com, Hosseinpoor.masood@yahoo.com
[2] Dept. of Geotechnics-Transportation and Surveying, Faculty of Civil Engineering, Shahrood University of Technology, Iran - sgharachelo@shahroodut.ac.ir

KEY WORDS: DInSAR, Land Deformation, Land Use, Garmsar, Alluvial Fan, Sentinel-1.

ABSTRACT:

Differential Synthetic Aperture Radar Interferometry (DInSAR) allows displacements to be detected with millimeter accuracy as well as more advanced methods, such as Persistent Scatterer Interferometry (PSI). Sentinel-1 data have been collected systematically under the COPERNICUS program at a high temporal resolution with global coverage, helping us to build a wide user community and develop miscellaneous SAR-based applications. In the Garmsar alluvial fan, the long-term groundwater overexploitation due to agricultural and urban demands, the utilization of urban space, and erosion have led to land deformation. In this study, the analysis of land subsidence in Garmsar fan was assessed by using the Differential Interferometric Synthetic Aperture Radar (DInSAR) technique based on 20 Sentinel-1 SAR images from January 2019 to June 2022. Distinct variations of land subsidence were found in the study regions however, it can be seen in most land use types. The maximum annual land subsidence rate has occurred in urban areas with an average rate of 95.2 mm/year from 2019 to 2022. Analysis showed that serious land subsidence mainly occurred in the following land use types: urban areas, agricultural lands, and bare lands.

1. INTRODUCTION

Differential Interferometric Synthetic Aperture Radar (DInSAR) is a satellite-based remote sensing technique that can be used to measure small displacements of the Earth's surface by removing or diminishing all the contributors to the interferometric phase except the displacement (Zhou et al., 2017). Differential SAR Interferometry (DInSAR) was initially used to measure the deformation of the land surface through the interpretation of Interferograms, with a combination of digital elevation models (DEM) to remove the topographic contributions. DEMs were obtained with the SAR Interferometry by using one or two additional SAR images and it was called three, or four-pass interferometry (Mancini et al., 2021).

Land subsidence is a gradual, long-term geological catastrophe that can be brought on by both natural and human-caused compaction (Zhang et al., 2014). In actuality, excessive groundwater extraction is the most frequent cause of land subsidence (Dehghani Bidgoli et al., 2021). Measuring ground deformation is key to understanding the ground response to groundwater overexploitation, land use change, natural hazards, etc. Land subsidence has become a global issue threatening our environment.

Like any other remote-sensing method, Differential Interferometric Synthetic Aperture Radar (DInSAR) has drawn a lot of interest in the field of monitoring subsidence since it can assess ground deformation. InSAR, on the other hand, detects deformation between a satellite and an object in the line of sight in a single dimension (LOS). SAR must be used with other methods, such as GNNS or leveling, in order to obtain 3D deformation components.

Several approaches have been used to detect and measure land subsidence caused by groundwater over-extraction such as traditional levelling survey, extensometer, numerical modelling of the aquifer, and global positioning system (GPS). The conventional methods usually measure displacement point by point. Therefore, they are inadequate to map the spatial variability of land subsidence which is largely driven by different land cover types and the spatial heterogeneity of the aquifer (Ahmad et al., 2019).

Compared with other techniques, traditional levelling, and GPS, Interferometric Synthetic Aperture Radar (InSAR) techniques have been successfully applied to study land deformation using multiple SAR images with a wide spatial range and millimeter-scale precision (Zhou et al., 2017).

The generated deformation maps can provide crucial information about the magnitude and spatial distribution of subsidence, and therefore the critical zones can be monitored easily to implement the remedial measures. Land subsidence due to groundwater abstraction is mainly controlled by the spatial pattern of groundwater consumption revealed by the land use types and the physical properties of the hydrogeological formation of the area (Ahmad et al., 2019).

Land subsidence characteristics in various land use types were investigated in Beijing Plain, China using InSAR techniques based on TerraSAR-X images over a 5-year period. The analysis showed that the land subsidence mainly occurred in

* Corresponding author

water areas and wetlands, paddy fields, upland soils, vegetable lands, and peasant-inhabited lands. The land subsidence in this area increased with the decrease in groundwater levels (Zhou et al., 2017). Land use change in the Vietnamese Mekong delta and its relationship with subsidence based on a 20-year time series was studied using Landsat-5 and InSAR-derived subsidence rates by previous studies. Results for the land use change sequences agreed well with the InSAR-derived subsidence rates, confirming the strong relation between land-use history and subsidence (Minderhoud et al., 2018). Quetta valley, Pakistan, has experienced land subsidence due to excessive groundwater extraction for irrigation and domestic supply. Ahmad et al., utilized Sentinel-1 and Sentinel-2 data to categorize the spatial distribution of land subsidence in 2014-2016. The results revealed that during the study period, the entire area suffered from varying degrees of accumulated land subsidence. The land subsidence was linearly proportional to the depth and depletion of groundwater observed at four piezometers located in the study area. The land subsidence over the study area showed a high correlation with land covers; e.g., the urban area and orchard vegetation with a large amount of groundwater abstraction showed an excessive amount of cumulative land subsidence (Ahmad et al., 2019).

Many of the major deltas in the world have gone through significant changes during the past decades. As as example, in the Southeast Asia, the Vietnamese Mekong delta stands out as hotspot of anthropogenic land-use change. These deltas can experience change in irrigation system, progressively becoming urbanized, with expanding networks which lead to fast-growing settlements (Minderhoud et al., 2018).

The land subsidence phenomenon is happening in most delta systems because deltaic sediments are highly compressible and susceptible to significant natural compaction during deposition and subsequent soil formation. The land subsidence is mainly due to human activities are widely recognized in deltas. Subsidence can be amlified by direct loading of the delta surface, both by natural material, such as water and sediment, and by manmade artifacts, like buildings and infrastructure. Also, the drainage of wetlands to prepare for agricultural use leads to a lowering of the phreatic water table, causing compaction in the subsoil. The organic material decomposition (oxidation) causes additional volume reduction. Also, the extraction of groundwater from deeper aquifers, to meet the increasing freshwater demands of rapidly urbanizing areas and agriculture, can lead to aquifer-system compaction.

Water Scarcity has affected the Garmsar alluvial fan due to its dry climate. However, it is one of the most important plains in the country with traditional agriculture has been modernized in recent years. Garmsar has a special economic and industrial landscape due to its proximity to Tehran as the capital city. In the past decades, rapid industrial and agricultural development in the region accompanied by rapid population growth and an increase in water demand, have led to an increase in the withdrawal of groundwater resources annually dropping groundwater aquifers level (Dehghani Bidgoli et al., 2021).

In this research, the DInSAR method was applied to obtain land deformation information in the Garmsar alluvial fan based on Sentinel-1 data from 2019 to 2022. The land use data of Garmsar alluvial fans have been assessed to examine the relationship between land use and subsidence in this area.

2. METHODOLOGY

2.1 Study Area

The study area (Figure 1) is a typical area in the northern part of the central desert of Iran with arid and semi-arid climates in hot summers and cold winters (Gharechelou et al., 2020). Garmsar plain has a total area of 320km^2 lays on the southern margin of Alborz and in the west of Semnan province (Dehghani Bidgoli et al., 2021).
The annual evapotranspiration in this area is 3200 mm, while the average annual rainfall is 140 mm (Gharechelou et al., 2020). The elevation of this area varies between 800 and 900 m above sea level. The groundwater in this area is mainly exploited by deep wells for agricultural lands and household purposes.
After leaving the southern Alborz Mountains, the Hablehrood River forms this plain at the foot of the mountain and in the north of the desert. This alluvial plain has always been affected by water scarcity due to its dry climate. However, it is one of the most important plains in the country in which traditional agriculture has been modernized in recent years.

Over the past decades, rapid industrial and agricultural development in this region, accompanied by rapid population growth which has led to an increasing water demand and groundwater resources extraction, have caused an annual dropping of groundwater level in aquifers 1.3 m (Dehghani Bidgoli et al., 2021)

Excessive groundwater abstraction, low rainfall, and high evaporation are the most important factors of desertification in this region.

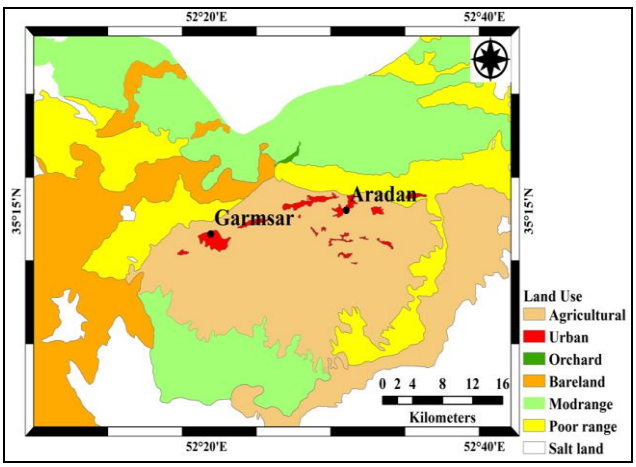

Figure 1. Location of the study area in Iran, based on land use map

2.2 SAR Data

The Sentinel-1 satellite was launched in 2014 by ESA based on Sentinel's satellites family program. The Sentinel–1 constellation of two identical SAR satellites (Sentinel-1 A and Sentinel-1 B) is the only operational mission providing global SAR data in a systematic and near real time. It also has a number of merits. First, it can image the same target location every 6 days with the two satellites. This is a significant improvement in the satellite revisit time. Secondly, it covers the globe with predefined observational scenarios periodically published and archived by the ESA. Furthermore, it has

enhanced spatial and radiometric resolution. Finally, the time interval between the image acquisition and its dissemination to the public can be even 1 day (Ahmad et al., 2019).

It has a revisiting time of 12 days and operates in the C-band of HH, VV, HV, and VH polarizations. The satellite carries a C-band Synthetic Aperture Radar which will provide images in all light and weather conditions. The land deformation in this study is analyzed using 20 Sentinel-1 SAR images acquired in Single Look Complex (SLC) Level-1 from descending track between the years 2019 and 2022. The specification of acquisition SAR data is presented in Table (1).

Acquisition date	Image Type	Polarization	Direction
20190110	SLC - L1	VV	Descending
20190323	SLC - L1	VV	Descending
20190814	SLC - L1	VV	Descending
20191001	SLC - L1	VV	Descending
20191224	SLC - L1	VV	Descending
20200222	SLC - L1	VV	Descending
20200422	SLC - L1	VV	Descending
20200621	SLC - L1	VV	Descending
20200820	SLC - L1	VV	Descending
20201019	SLC - L1	VV	Descending
20201230	SLC - L1	VV	Descending
20210204	SLC - L1	VV	Descending
20210417	SLC - L1	VV	Descending
20210616	SLC - L1	VV	Descending
20210815	SLC - L1	VV	Descending
20211014	SLC - L1	VV	Descending
20211213	SLC - L1	VV	Descending
20220130	SLC - L1	VV	Descending
20220223	SLC - L1	VV	Descending
20220424	SLC - L1	VV	Descending
20220611	SLC - L1	VV	Descending

Table 1. The characteristics of data sets

The selected IW-SLC images used in the present study were processed using the Sentinel Application Platform Sentinel-1 toolbox (SNAP). The software was used to perform the Interferometric process including master image selection, topographic phase removal, and Interferogram generation. A 30-m SRTM DEM (available at https://earthexplorer.usgs.gov/) was used to remove the topographic phase. After producing the Line of Sight (LOS) displacement, the cumulative displacement map was produced to investigate the land deformation and achieve a better comprehension of the data and further analysis.

2.3 Data Processing

In DInSAR, relative distances are precisely measured by comparing the phases of two photos obtained over the same region at different periods. The DInSAR technique can be divided into two groups, namely cumulative DInSAR and consecutive DInSAR. The former uses a fixed master image and the selection of a slave image (such as 1-2, 1-3, 1-4,..., n) afterward describes the cumulative DInSAR technique. This method is particularly susceptible to temporal decorrelation, which typically gets worse in the slave images that follow, while the latter utilizes differential interferograms of nearby SAR acquisitions that are computed and added together to yield full time-series interferometric results (e.g., 1-2, 2-3, 3-4,..., n-1,n). This method minimizes temporal decorrelation by using short temporal baselines (6 days when Sentinel-1A and Sentinel- 1B are combined). This technique, however, have certain drawbacks. If any errors (residual terrain, atmospheric delay, and other phases error) are found in any of the calculated displacements in the interferograms, they propagate in the ensuing time-series deformation outcomes in the accumulation process.

In this study, consecutive DInSAR is used to overcome the mentioned drawbacks of conventional methods. The processing of data was performed using SNAP. The subswath IW3 of the Sentinel–1 IW–SLC VV polarized images acquired in relative orbit number 137 are selected because this subswath covers the study area. The precise orbit files, that provide accurate information about the location of the satellite are applied to the images to determine the accurate satellite position at the time of image acquisition (Ahmad et al., 2019).

The master and slave images are co-registered before the interferogram formation. It involves resampling the slave images with respect to the grid system of the master image so that each interferogram constitutes the same geolocation precisely. In data processing, co-registered paired images are used to create a differential Interferogram, which is an image displaying the phase change brought on by deformation. Following this, a total number of 19 interferograms were generated.

Data coherence is then calculated. Coherence is an important metric of data quality that assesses how similar the signals are in the paired images. After co-registration, the interferograms were generated and the simulated phase corresponding to the topography was removed from the SRTM DEM with 30-m pixel resolution. Coherence is measured on a scale from zero to one, with zero denoting no similarity and poor data quality and one denoting complete similarity and excellent data quality. Absolute interferometric phases are established after the Interferogram is spatially filtered to remove noise. The phase unwrapping was performed using the Statistical-cost, Network–flow Algorithm for Phase Unwrapping (SNAPHU).

The absolute phases are used to estimate displacements. The line of sight (LOS) vector, which contains both horizontal and vertical displacement, is used to quantify displacements. The features of the sensor and satellite, as well as the surface and deformation properties, determine how effectively DInSAR may be used to measure subsidence (Wempen et al, 2017).

Data decorrelation and phase saturation may reduce the DInSAR's ability to accurately quantify subsidence. Significant changes in the surface properties or the imaging characteristics over time are what generate data decorrelation. Phase saturation can be brought on by large deformation gradients. DInSAR cannot directly measure the absolute displacements when the phases are saturated.

In this investigation, data were matched across the shortest time frames possible to reduce the impact of temporal variations and phase saturation. The differential interferograms were filtered to reduce atmospheric artifacts, and those that had obvious

atmospheric errors were taken out of the stack. The data were then added together to estimate the subsidence over larger time frames. The DInSAR process can be seen in Figure 2.

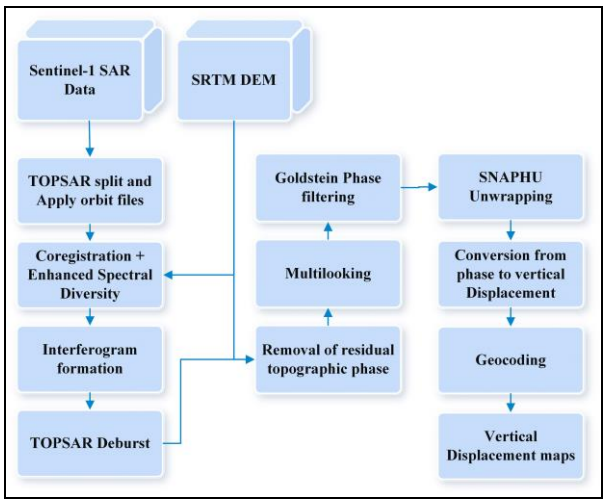

Figure 2. The conventional DInSAR workflow

2.4 Land Use Data

To investigate the relationship between land subsidence and land use types, the Land use map prepared by the Iranian Institute of Water and Soil (http://www.swri.ir/) using Landsat images. These data were used for the extraction of land deformation values in various land use types.

3. RESULT AND DISCUSSION

A total of 19 Interferograms of the study area were generated to monitor land subsidence during the 2.5 years. Figure (2) shows the displacement map of the Garmsar alluvial fan using the DInSAR method. The deformation information is along the SAR's line-of-sight (LOS) direction, therefore, the subsidence results were projected along with a vertical direction with respect to the corresponding incidence angles. The colour scale bar covers a range of 101 mm uplift and maximum subsidence of 416 mm occurring during the period in the study area.

The study was focused on four main land use types: urban areas, agricultural lands and orchards, bare lands, and rangelands. While comparing the land use (Figure 1) and the land subsidence map of Figure 3, it can be clearly seen that the land use types have a strong impact on land subsidence. The land subsidence in the agricultural areas and urban areas seems different than that of the other land use types (the most accumulated deformation and the most subsidence in the areas, respectively).

Although subsidence has occurred in most parts of the region, it can be clearly seen that the majority of subsidence has occurred in the southern and western parts of the study area. There has been a linear area indicating moving away from the satellite, which is the erosion that happened in the river bed. The accumulated subsidence resulting in different subsidence rates across the area due to different land use types and during the study period is further compared, which shows that land use type is a clear indicator of the amount of groundwater use in the study area.

According to previous studies, moving from the northwest towards the southeast of the Garmsar plain, the decline in groundwater decreases, which is aligned with the same pattern as subsidence in the area (Dehghani Bidgoli et al., 2020). The gradual spatial expansion of the red regions shows that the land subsidence is steadily propagating to the adjoining urban areas, especially, Garmsar city.

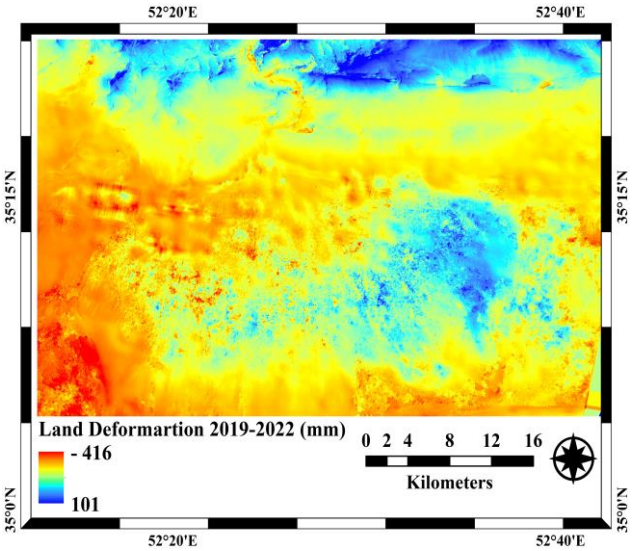

Figure 3. The spatial distribution and critical zone of Cumulative displacement detected by DInSAR analysis

While comparing the land use map (Figure 1) and the land subsidence map in Figure 3, it can be seen that the land use types influence land subsidence. The accumulated subsidence resulting in different subsidence rates across the area due to different land use types during the study period is further analyzed to investigate the relationship between land use and land deformation.

The urban area and orchards which is analogous to the alluvial plain show a more significant and monotonic tendency of subsidence with a mean rate of 95.2 and 81.2 mm/year; the deformation in these areas indicates that land subsidence is mostly caused by groundwater consumption, and is more consistent than range lands, with a recorded deformation rate of 68.8 mm/year (Table 2).

According to the table, the subsidence only between bare land and the urban area land use is not significantly different from each other at less than 5% significance level (4%), while the subsidence between all other land use types is significantly different from each other.

	Bare land	Urban area	Range land	Agricultural area
Accumulated deformation (mm)	-237	-238	-172	-203
Subsidence rate (mm/year)	-94.8	-95.2	-68.8	-81.2
Maximum value of Deformation (mm)	-75	-141	55	-62
Minimum value of Deformation (mm)	-336	-179	-320	-333

Table 2. Characteristics of land use-based land deformation

The bare lands do not receive any regular irrigation water, which makes the magnitude of soil shrink significant. The deformation in range land areas is sought to be caused by erosion, and a small area showing uplift is due to vegetation growth.

It is a known fact that subsidence is mainly caused by groundwater overexploitation, and the volume of water extracted for agricultural use is more than for urban use. Also, the agricultural area in the fan experienced significant subsidence.

Unfortunately, there is not any substantial source of surface water in the study area. Furthermore, evapotranspiration is significantly higher than precipitation; therefore, it is a valid justification that the anthropogenic activities are largely supplied by pumping groundwater which leads to land subsidence, and this tendency of land subsidence is detected very well by the SAR analysis. As can be seen, the maximum subsidence that has occurred in the agricultural areas is approximately double than that of urban areas.

To achieve a better estimation, 100 random points were generated in each land use type. Then, using extract values to points, the figure for deformation in each point was extracted from the displacement map. Then, the Nan values were removed, and finally, 98 selected points in each area were used to generate a box and whisker plot according to Figure 4. As can be seen, urban and agricultural areas were affected more than two others by land subsidence and their absolute value was more than that of rangelands and bare lands.

Regarding rangelands, the deformation in these areas varied more than in others due to differences in the intensity of erosion and vegetation. One of the random points in this class indicates a little uplift in the class. Looking at bare lands, it can be seen that the land subsidence varied between approximately 75mm and around 200mm. Figure 3 is a confirmation of the influence of groundwater consumption and land use on land deformation.

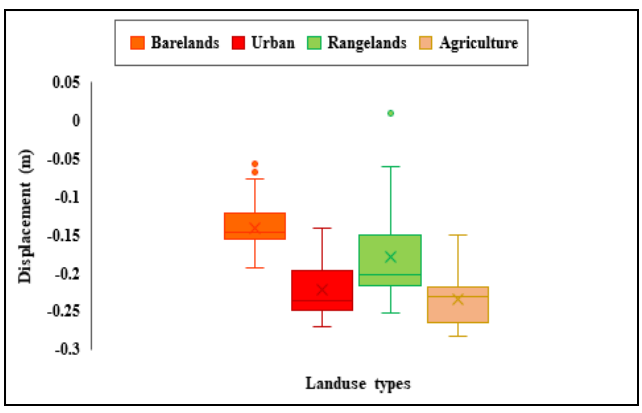

Figure 4. Box and Whisker plot for the variation of random points in the deformational areas according to the four selected land use types; Bare lands, Urban areas, Rangelands, and Agricultural areas

4. CONCLUSION

The present study indicates that the Sentinel–1 satellite data can be employed as a valuable tool to identify the spatiotemporal trend of land subsidence in the study area. DInSAR can generate data with a high spatial and temporal resolution for subsidence monitoring. It has the potential to characterize geographical characteristics of subsidence as well as give rapid and reliable reports on the amount, scope and pace of subsidence. The DInSAR method was employed to assess the relationship between land deformation and land use types in Garmsar alluvial fan. During the 2.5 years, the study area experienced a varying level of land subsidence with a minimum mean rate of 172 mm and maximum mean rate of 238 in range lands and urban areas, respectively. Results showed that land subsidence mostly occurred in urban area, which is affected by human activities, and the subsidence increases moving from east towards the western parts of the plain. Measuring and mapping the land deformation varying with different land use types could be challenging for the traditional approaches based on point measurements or topographic levelling.

The present study also shows that the Sentinel–1 satellite data can be freely used as a valuable tool for identifying the spatio-temporal land subsidence trend in the study area. Furthermore, quantifying and mapping the land subsidence according to different land use types could be a challenging job for the traditional, based on point measurements, approaches or topographic levelling. The satellite data and the data processing software is provided free of cost by the ESA and no financial cost was invested in this regard. We expect our methodology can be used to study similar risks in other locations across the world and to better manage the groundwater resources to avoid land subsidence. We would also recommend using Sentinel-2 data to investigate the land cover maps in the study area which would be updated and could also be pre-processed in open-source SNAP software.

ACKNOWLEDGMENTS

The authors would like to acknowledge the ESA Copernicus data hub for the provision of Sentinel–1 data. Also, we are thankful to the reviewers whose reviews and comments greatly improve the quality of this work.

REFERENCES

Ahmad, W., Choi, M., Kim, S. and Kim, D., 2019: Detection of land subsidence and its relationship with land cover types using ESA Sentinel satellite data: a case study of Quetta Valley, Pakistan. *Int. J. Remote Sens.*, 40(24), 9572-9603. doi.org/10.1080/01431161.2019.1633704

Dehghani Bidgoli, R. and Yazdani, M.R., 2021: Survey and visualization of land subsistence caused by groundwater depletion using Sentinel-1A IW TOPS Interferometry. *Nat. resour. environ,* 9(1), pp.107-116.doi.org/10.1016/j.jhydrol.2021.127329

Gharechelou, S., Tateishi, R. and Johnson, B.A., 2020: Mineral Soil Texture–Land Cover Dependency on Microwave Dielectric Models in an Arid Environment. *Land*, 9(2), 39. doi.org/10.3390/land9020039

Mancini, F., Grassi, F. and Cenni, N., 2021: A workflow based on SNAP–StaMPS open-source tools and GNSS data for PSI-Based ground deformation using dual-orbit sentinel-1 data: Accuracy assessment with error propagation analysis. *Remote Sens.*, 13(4), p.753. doi.org/10.3390/rs13040753

Minderhoud, P.S.J., Coumou, L., Erban, L.E., Middelkoop, H., Stouthamer, E. and Addink, E.A., 2018: The relation between land use and subsidence in the Vietnamese Mekong delta. *Sci. Total Environ.* 634, pp.715-726. doi.org/10.1016/j.scitotenv.2018.03.372

Wempen, J.M., and McCarter, M.K., 2017: Effective application of synthetic aperture radar interferometry for monitoring mine subsidence in the mountain west United States. *SME Preprint No. 17-049. Englewood, CO: SME*. doi.org/10.1016/j.ijmst.2019.12.011

Zhang, Y. Q., H. L. Gong, Z. Q. Gu, R. Wang, X. J. Li, and W. J. Zhao. 2014. Characterization of Land Subsidence Induced by Groundwater Withdrawals in the Plain of Beijing City, China. *Hydrogeol. J,* 22 (2): 397–409. doi:10.1007/s10040-013-1069-x.

Zhou, C., Gong, H., Chen, B., Li, J., Gao, M., Zhu, F., Chen, W. and Liang, Y., 2017: InSAR time-series analysis of land subsidence under different land use types in the Eastern Beijing Plain, China. *Int. J. Remote Sens.*, 9(4), 380. doi.org/10.3390/rs9040380